

AD-A212 497

TIC

DOCUMENTATION PAGE

SEP 20 1989

1a. SECURITY CLASSIFICATION AUTHORITY Unclassified			1b. RESTRICTIVE MARKINGS	
2b. DECLASSIFICATION/DOWNGRADING SCHEDULE			3. DISTRIBUTION/AVAILABILITY OF REPORT Approved for Public Release; Distribution Unlimited	
4. PERFORMING ORGANIZATION REPORT NUMBER(S) GL-TR-89-0252			5. MONITORING ORGANIZATION REPORT NUMBER(S)	
6a. NAME OF PERFORMING ORGANIZATION Geophysics Laboratory (AFSC)		6b. OFFICE SYMBOL (If applicable) PHS		7a. NAME OF MONITORING ORGANIZATION
6c. ADDRESS (City, State, and ZIP Code) Hanscom AFB Massachusetts 01731-5000			7b. ADDRESS (City, State, and ZIP Code)	
8a. NAME OF FUNDING/SPONSORING ORGANIZATION		8b. OFFICE SYMBOL (If applicable)		9. PROCUREMENT INSTRUMENT IDENTIFICATION NUMBER
8c. ADDRESS (City, State, and ZIP Code)			10. SOURCE OF FUNDING NUMBERS	
			PROGRAM ELEMENT NO 62201F	PROJECT NO 2311
			TASK NO G3	WORK UNIT ACCESSION NO. 12
11. TITLE (Include Security Classification) The Relation Between Convection Flows and Magnetic Structure at the Solar Surface				
12. PERSONAL AUTHOR(S) G.W. Simon, L.J. November*, L.W. Acton*, A.M. Title*, T.D. Tarbell*, K.P. Topka*, R.A. Shine*, S.H. Ferguson*, N.O. Weiss*, H. Zirin*				
13a. TYPE OF REPORT Reprint		13b. TIME COVERED FROM TO		14. DATE OF REPORT (Year, Month, Day) 1989 September 12
15. PAGE COUNT 7				
16. SUPPLEMENTARY NOTATION * See Reverse for Author Affiliation Reprinted from Adv. Space Res. Vol. 8, No. 11. pp(11)133-(11)139, 1988				
17. COSATI CODES			18. SUBJECT TERMS (Continue on reverse if necessary and identify by block number)	
FIELD	GROUP	SUB-GROUP	Solar Granulation; Solar Convection; Solar Magnetism	
19. ABSTRACT (Continue on reverse if necessary and identify by block number) We describe recent results from the comparison of data from the Solar Optical Universal Polarimeter instrument on Spacelab 2 and magnetograms from Big Bear Solar Observatory. We show that the Sun's surface velocity field governs the structure of the observed magnetic field over the entire solar surface outside sunspots and pores. We attempt to describe the observed flows by a simple axisymmetric plume model. Finally, we suggest that these observations may have important implications for the prediction of solar flares, mass ejections, and coronal heating.				
20. DISTRIBUTION/AVAILABILITY OF ABSTRACT <input type="checkbox"/> UNCLASSIFIED/UNLIMITED <input checked="" type="checkbox"/> SAME AS RPT <input type="checkbox"/> DTIC USERS			21. ABSTRACT SECURITY CLASSIFICATION Unclassified	
22a. NAME OF RESPONSIBLE INDIVIDUAL Claire Caulfield			22b. TELEPHONE (Include Area Code) (617) 377-4555	22c. OFFICE SYMBOL SULLP

89 9 19 08 6

Cont of Block 16:

G. W. Simon,* L. J. November,** L. W. Acton,***
A. M. Title,*** T. D. Tarbell,*** K. P. Topka,***
R. A. Shine,*** S. H. Ferguson,*** N. O. Weiss† and
H. Zirin‡

*Air Force Geophysics Laboratory, Sunspot, NM 88349, U.S.A.

**National Solar Observatory, Sunspot, NM 88349, U.S.A.

***Lockheed Palo Alto Research Laboratories, 3251 Hanover St., Palo
Alto, CA 94304, U.S.A.

†DAMPF, University of Cambridge, Silver Street, Cambridge CB3 9EW,
U.K.

‡California Institute of Technology, Pasadena, CA 91125, U.S.A.



Accession For	
NTIS GRA&I	<input checked="checked" type="checkbox"/>
DTIC TAB	<input type="checkbox"/>
Unannounced	<input type="checkbox"/>
Justification	
By _____	
Distribution/	
Availability Codes	
Dist	Avail and/or Special
A-1	20

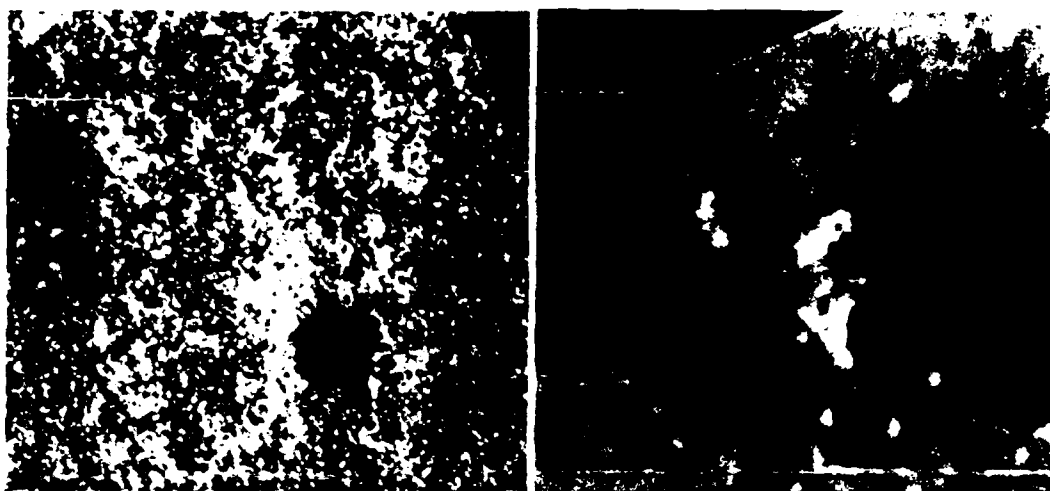


Fig. 1. Solar region analyzed in this study. (Left) SOUP white-light photo showing granulation, sunspot, and pores. (Right) Corresponding magnetogram from BBSO in which dark and light regions indicate opposite magnetic field polarity.

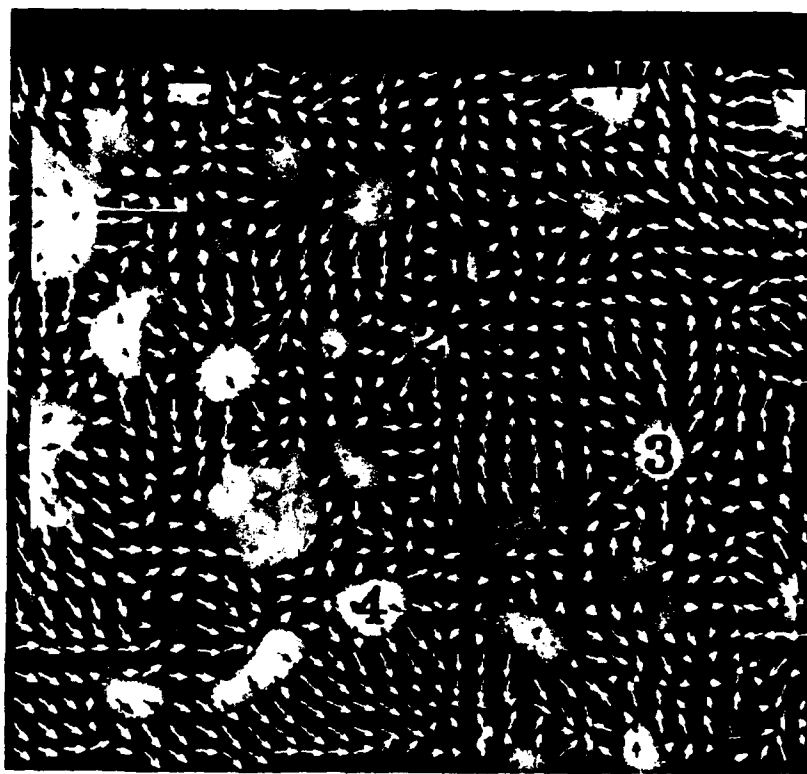


Fig. 2. Superposition of observed horizontal flow vectors and the divergence calculated from this velocity field. Bright regions are sources (four such features have been dark). The area shown is the same as in Fig. 1.

The major significance of this result becomes apparent if one considers the relation between these flows and the Sun's surface magnetic field. We find [2] that magnetic features follow the same paths as the velocity corks. The well-known magnetic network which outlines the boundaries of supergranules is co-spatial with the cork distribution 8 to 16 h after the corks start from a uniform distribution. Some magnetic features converge to the same sink points as the corks, but much of the magnetic structure apparently prefers to remain as a network pattern.

The phenomena we have just described can best be seen by high speed cinematography. However, we summarize these results in Figures 3 and 4. In Figure 3 (left) we show the flow field of Figure 2 superposed on the magnetic field of Figure 1 (right). Figure 3 (right) is the superposition of the

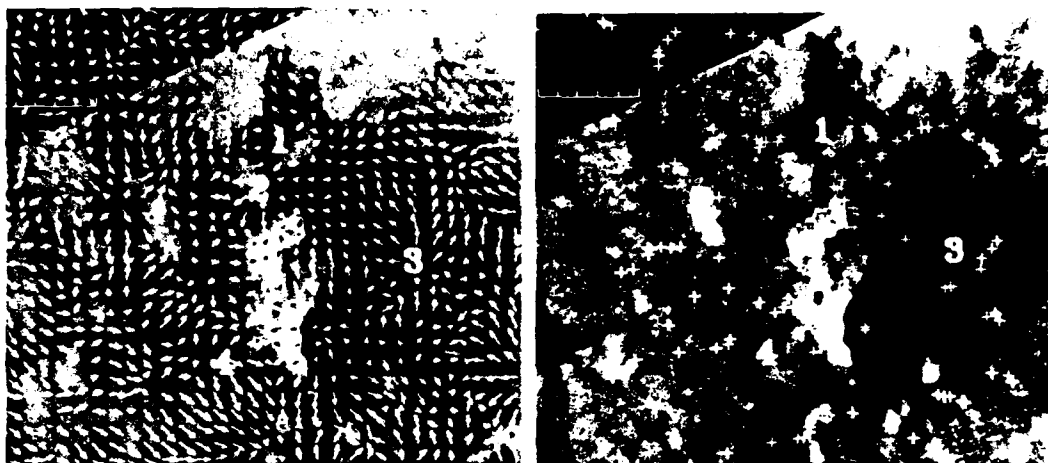


Fig. 3 Comparison among magnetic field structure, flow vectors, and velocity corks, for the area shown in Fig. 1 and Fig. 2. Superposition of magnetic field and (left) velocity vectors, (right) corks after 12 h.

magnetic field and the corks after 12 h. If one compares these two photographs, one can see easily that both the corks and the magnetic features concentrate wherever arrows indicate converging flow. To demonstrate this phenomenon more clearly, we have enlarged five small sections of Figure 3 and display them in Figure 4. Each of these examples illustrates the same point: Wherever there is an opposing flow field, the magnetic field becomes concentrated. Except in the regions of strongest field (sunspots and pores), the observations indicate that the field apparently does what the velocity field "dictates". That is, the data suggest the following relation between the magnetic and kinetic energy densities at that level in the solar atmosphere where gas motions determine the magnetic structure we see at the surface:

$$\frac{1}{2} \rho v^2 > \frac{B^2}{8\pi} \quad (1)$$

in which v = gas velocity, B = magnetic density, and ρ = gas density. This relevant level is probably below the visible surface, since the observed concentrations of B (1000–1500 gauss), measured 100–200 km above the surface, are far stronger than the left-hand term of equation (1) can provide at this level, according to the limit placed by equipartition of energy (equation (1) with an $=$ sign). Note, however, that numerous theoretical studies [8,9,10,11] have shown that it should be possible to amplify the magnetic field to values much larger than the equipartition value, so it is by no means certain that the surface motions are unable to create the observed flux concentrations.

There may be important implications of these observations. By measuring the velocity fields, we hope to understand where magnetic fields will concentrate and be subjected to stresses. The SOUP velocities also show [5] vortical (twisting) motions strong enough that the gas makes a full 360° turn in 2 to 3 h. If the footpoint of a magnetic flux tube embedded in such a flow pattern "obeys" this spiraling motion as it seems to follow the diverging and converging flows discussed above, it could become twisted into an unstable magnetic configuration. These observations indicate that it may become possible to predict those places on the Sun's surface most likely to produce solar flares, mass ejections, and coronal heating.

MODELING

Attempts are now underway [12] to model these flows by simple potential functions which satisfy the continuity equation

$$\nabla \cdot (\rho \mathbf{v}) = 0 \quad (2)$$

A function which satisfies equation (2) and represents radial horizontal outflow from an isolated source is:

$$\mathbf{v}(r) = V \left[\frac{r}{R} \right] e^{-\left[\frac{r}{R} \right]^n} \quad (3)$$

in which case the flow divergence (proportional to the vertical velocity) is

$$\Delta = \frac{V}{R} \left[2 - n \left(\frac{r}{R} \right)^n \right] e^{-\left(\frac{r}{R} \right)^n} \quad (4)$$

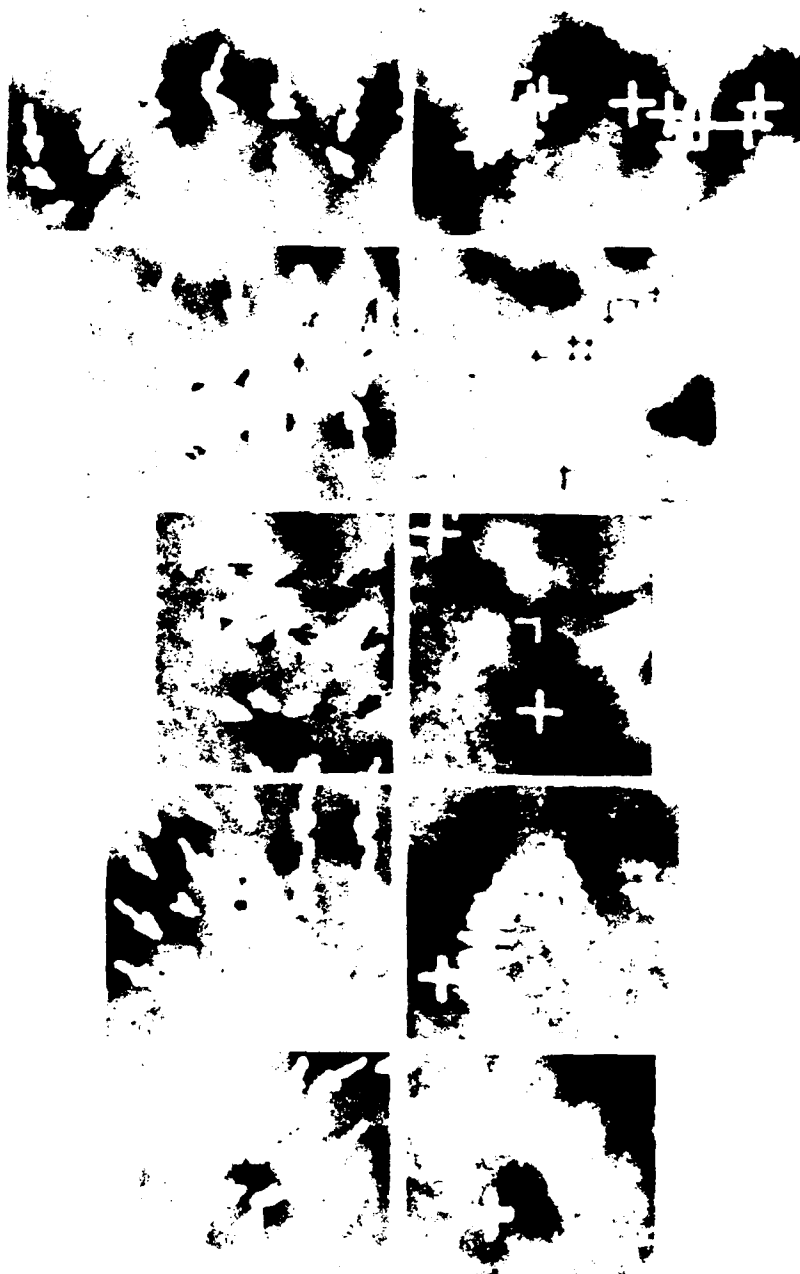


Fig. 4. Enlargements of five small sections of Fig. 3. In each case, the velocity vectors point toward a concentration of magnetic field and corks. The five areas shown run from top to bottom in Fig. 3. Particularly interesting are (second from top) a collision between outflow from the mesogranule labeled 2 and the sunspot, (third from top) a collision between outflow from the supergranule labeled 4 and the sunspot, and (bottom) convergence to a sink point. In this last example, the single cork visible is actually a superposition of five corks which have already converged at this site.

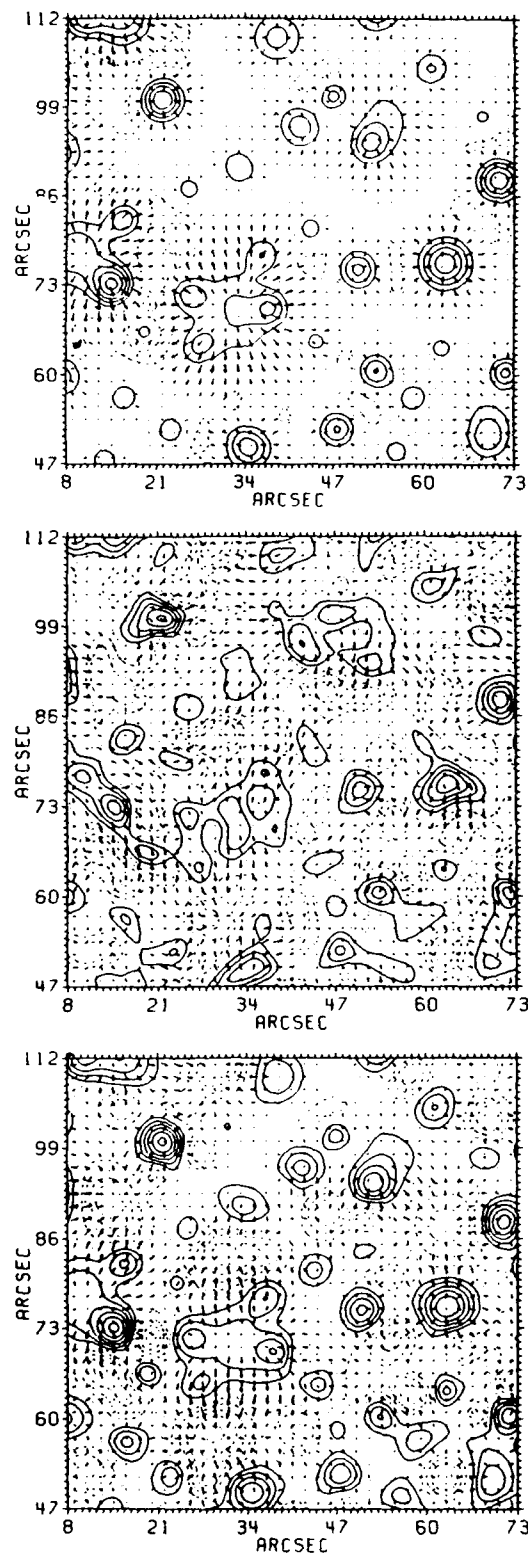


Fig. 5. Comparison of SOUP velocity vectors and divergence contours with those of axisymmetric plume model. (Center) SOUP data. (Top) Model containing only axisymmetric sources. (Bottom) Model having both sources and sinks. Solid lines are positive contours, dashed lines are negative contours, and short dashes (dots) are zero contours.

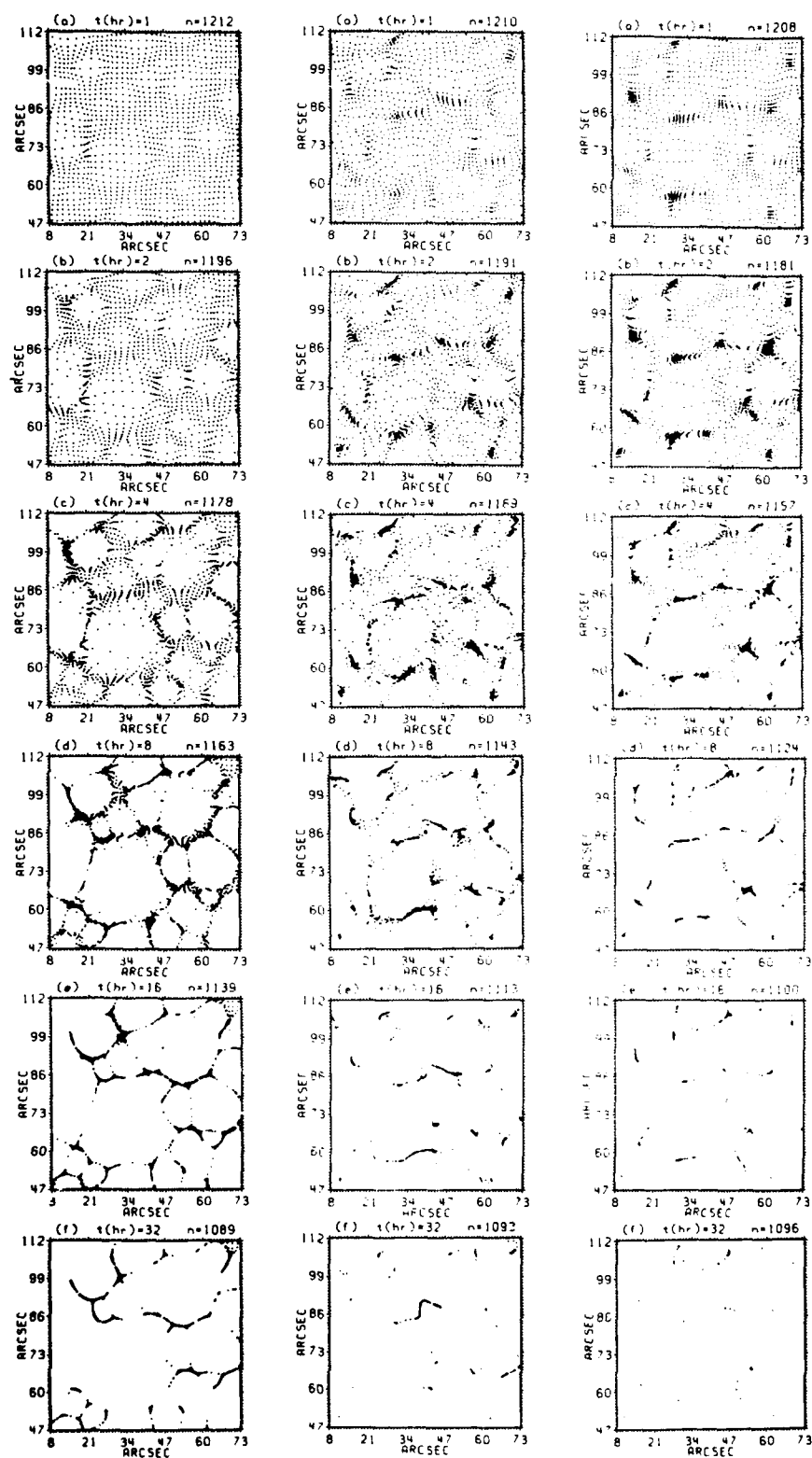


Fig. 6. Cork positions 1, 4, 8, 16, and 32 h after starting from a uniform distribution. Time increases downward in each column. (Center) SOUP data. (Left) Model with sources only. (Right) Model with both sources and sinks.

Each outflow in the observed data can be represented by such functions, where R is determined from the point where the observed Δ goes to zero and V is the central "strength" of the divergence maximum. We have found [12] that $n=2$ works satisfactorily for most of the data analyzed. We then superpose all the observed maxima of Δ and compare the resulting model velocity field with the real data. Such a comparison is shown in Figure 5, with the modeled flow at the top, and the SOUP data in the center, for a 65" by 65" section of the SOUP image. Although the real data show distorted divergence contours, twisting and streaming motions, and convergence into sinks, none of which is included in the simple axisymmetric source model described by equations (3) and (4), nevertheless the two pictures agree in many details. A much closer comparison between SOUP and model data results if we include in the model the observed sinks. In this case we fit both sources and sinks with equation (4), but of course the strength V has a negative value for a sink. The resulting flow pattern is shown in Figure 5 (bottom).

A more severe test of the model is to compare the real and the model cork flows, which we do in Figure 6. The cork positions are shown 1, 2, 4, 8, 16, and 32 h after starting from a uniform distribution. The area is the same as in Figure 5. It is clear that the addition of sinks (right-hand column) makes the model cork behavior look more like the actual SOUP data (center column). However, the sources-only model (left-hand column) also agrees well with the real data for the first 4 to 8 h. After that, the corks (much like the actual magnetic field) remain in a network configuration for many hours, while the SOUP corks and the corks in the model with sinks quickly converge to the sink locations. Further model studies are in progress.

In the absence at the present time of low-noise solar data from space, ground-based observations similar to those from SOUP are being obtained at the Swedish Solar Observatory at La Palma (Canary Islands, Spain) and at the National Solar Observatory (Sunspot, NM, USA). Such studies, together with improved modeling of the flows, should prove most interesting in the prediction of solar flares and mass ejections during the 1989-1991 maximum of solar cycle 22.

REFERENCES

1. Title, A., Tarbell, T., Simon, G. and the SOUP Team, *Adv. Space Res.* **6**, 253 (1986).
2. Simon, G., Title, A., Topka, K., Tarbell, T., Shine, R., Ferguson, S., Zirin, H. and the SOUP Team, *Ap. J.* **327**, 964 (1988).
3. Shine, R., Title, A., Tarbell, T., and Topka, K., *Science* **238**, 1264 (1987).
4. Title, A., Tarbell, T., Topka, K., Ferguson, S., Shine, R., and the SOUP Team, *Ap. J.*, in press (1988).
5. Simon, G., November, L., Zirin, H., Ferguson, S., Shine, R., Tarbell, T., Title, A., and Topka, K., *Adv. Space Res.* (COSPAR, Helsinki, July 1988, Paper 12.4.3), in press (1988).
6. November, L., *Appl. Optics* **25**, 392, 1986.
7. November, L. and Simon, G., *Ap. J.* **333**, in press (1 October) (1988).
8. Galloway, D. and Weiss, N., *Ap. J.* **243**, 945 (1981).
9. Proctor, M. and Weiss, N., *Rep. Prog. Phys.* **45**, 1317 (1982).
10. Galloway, D. and Proctor, M., *Geop. Ap. Fl. Dyn.* **24**, 109 (1983).
11. Nordlund, A., *Solar Phys.* **100**, 209 (1985).
12. Simon, G., and Weiss, N., *Ap. J.*, submitted (1988).